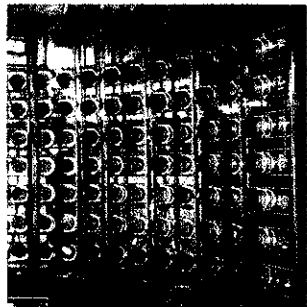
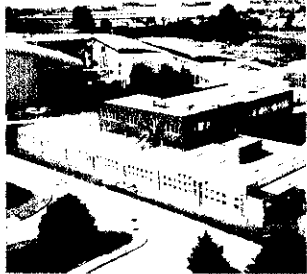


# LABORATOIRE DE PHYSIQUE CORPUSCULAI



## Design and performance of an RFQ cooler and buncher

J. Szerypo, G. Ban, Ch. Le Brun, P. Delahaye, D. Hennecart,  
E. Liénard, F. Mauger, O. Naviliat-Cuncic, B. Tamain

octobre 1999

LPCC 99-18

Rapport interne

CENTRE NATIONAL DE LA RECHERCHE SCIENTIFIQUE

INSTITUT NATIONAL  
DE PHYSIQUE NUCLÉAIRE ET DE PHYSIQUE DES PARTICULES

INSTITUT DES SCIENCES DE LA MATIÈRE ET DU RAYONNEMENT

UNIVERSITÉ DE CAEN

- U.M.R.6534 -

ISMRA - 6, Boulevard Maréchal Juin - 14050 CAEN CEDEX - FRANCE

Téléphone : 02 31 45 25 00 - Télécopie : 02 31 45 25 49

Internet : <http://caeinfo.in2p3.fr>

# Design and performance of an RFQ cooler and buncher

J. Szerypo<sup>1</sup>, G. Ban<sup>1</sup>, C. Le Brun<sup>1</sup>, P. Delahaye<sup>1</sup>, D. Hennecart<sup>2</sup>,  
E. Lienard<sup>1</sup>, F. Mauger<sup>1</sup>, O. Naviliat<sup>1</sup> and B. Tamain<sup>1</sup>

<sup>1</sup>Laboratoire de Physique Corpusculaire de Caen  
6, bd Maréchal Juin, 14050 Caen CEDEX

<sup>2</sup>Centre Interdisciplinaire de Recherche Ions Lasers  
bd Henri Becquerel, BP 5133, 14070 Caen CEDEX 5

## Abstract

Several new experiments, planned or in preparation at low energy radioactive beam facilities, require the cooling and bunching of radioactive beams. This may be performed with a radio-frequency quadrupole (RFQ) cooler and buncher, where the ions are cooled in a buffer gas while being guided by an oscillating RFQ field. This work describes the performance of such a device, which has been designed and studied in order to be extended for the cooling of light ions. The analysis requires extensive computer simulations, which are done with two approaches: the macroscopic and the microscopic. The latter approach is able to account for the RF-heating effect and the calculations were performed by the Monte Carlo method. The cooling formalism was extended to include a charge-exchange effect. The charge-exchange cross sections were calculated theoretically in a quantum-mechanical formalism for different ion-atom combinations. The simulations have shown in particular that for the cooling of  ${}^6\text{He}^+$  ions,  ${}^4\text{He}$  is excluded as buffer gas because of the resonant charge exchange processes which drastically decreases the transmission. On the other hand, the cooling of  ${}^6\text{He}^+$  ions with  $\text{H}_2$  as buffer gas appears as a promising solution. The most relevant cooler design parameters are proposed. A project of a complete system, including the deceleration, extraction and transfer sections, is presented.

## 1. Introduction

Ion trap systems coupled to low energy radioactive beam facilities open up new possibilities to measure spectroscopic and decay properties of exotic nuclei with unprecedented precision. The ions produced by different types of sources should first be cooled to achieve a high trapping efficiency. This process reduces both the longitudinal and the transverse emittances. The ions may eventually be bunched if they are to be injected in a Paul trap which requires the injection to take place only within a narrow phase window of the radio-frequency.

A widely spread scheme being considered at several laboratories for the cooling of radioactive beams is the so-called "buffer gas cooling". Most of the devices designed so far will apply this scheme for the cooling of medium mass to heavy ions using a light buffer gas which is generally helium. However, some experiments [1] do require the cooling of ions as light as  ${}^6\text{He}^+$  and the efficiency of the buffer gas cooling requires then a specific detailed analysis.

In this paper we analyze the performance of a general radio-frequency quadrupole (RFQ) cooler and buncher which has been designed in order to extend its cooling capabilities down to light ions with an acceptable transmission. The study assumes the characteristics of the radioactive ECR ion source in operation at the SPIRAL facility at GANIL and that the experiments are performed in a Paul trap installed beyond the RFQ cooler and buncher.

## 2. Methods for beam cooling

To cool a beam of particles means to act on this beam in such a way that all the particles tend to occupy the smallest volume in phase space. In other words, the cooling process should decrease the diameter, the divergence and the energy spread of the beam. The first two parameters are described by the transverse emittance. For a bunched beam, we talk rather about the longitudinal emittance instead of the energy spread. In the general case of ions, several cooling schemes exist. Stochastic cooling [2] and electron cooling [3] are generally used in storage rings. The ion trapping applications rely on resistive cooling [4], laser cooling [5], and buffer-gas cooling [6]. The first two are not applicable for short-lived radioactive ions

because of the relatively long time (in the range of seconds-minutes) needed for cooling. Moreover, laser cooling, which depends on the atomic energy level structure, is applicable so far to a limited range of species for which one can find the laser wavelength matching the level spacing. Therefore the most widely considered for singly charged radioactive ions is the buffer-gas cooling, due to its: short cooling times (of the order of some ms), relative simplicity and the great advantage of being universal. For a radioactive beam, buffer gas cooling is best performed using either a Penning trap or a device called a *RFQ ion guide*. The main features of both devices are described below.

## 2.1 Buffer gas cooling with an RFQ ion guide

Ions confined in a Paul [7] or Penning [8] trap can be cooled by introducing a light neutral gas such as H<sub>2</sub> or He. The ion motion is damped by collisions with the buffer gas atoms, in principle down to the temperature of the gas itself. Douglas and French [9] have extended this scheme to continuous beams. They used a two-dimensional version of the RFQ trap, called a *RFQ mass filter*, which consists basically of four parallel cylindrical rods. These authors demonstrated a dramatic gain in transmission through a small hole at the end of a tandem mass filter system simply by introducing buffer gas into one of the quadrupole sections. The mass filter focuses the ion beam onto the central axis alternately in each transverse direction, to overcome the diffusion that would otherwise occur during the transit of the ions in the gas. Thus the ions are guided along the axis defined by the quadrupole rod structure, being at the same time cooled by the buffer gas collisions, both in transverse and longitudinal directions. Such structure, usually operated at modest gas pressures (about 1 Pa), is called an *RFQ ion guide* or *RFQ cooler*. Since radionuclides are generally short-lived, the cooling process must be rapid. In principle, simply increasing the buffer gas pressure will increase the cooling rate. However, it cannot be increased beyond a certain limit since the operation of the electrical devices at high pressure may result in a voltage breakdown. Furthermore, continuous beams are generally transported at high kinetic energy, requiring a deceleration and subsequent re-acceleration of the beam. This means that the ion guide works on a floating high-voltage platform. Although stopping the accelerated beam directly in the gas would be in principle possible, the resulting secondary electrons would cause a discharge hindering the operation of the ion guide.

In several experiments under consideration the ions must be delivered to a Paul trap in the form of well defined bunches. The best place to perform such bunching is at the end of the RFQ cooler, where an axial electric potential well for the bunch containment can be created. This implies that the rod structure must be divided axially into segments, to which various DC potentials could be applied. Thus, the RFQ ion guide, or now the *RFQ cooler and buncher*, serves for both cooling and bunching purposes at the same time. Such radioactive beam cooling devices are presently in operation or under development at several laboratories:

- The RFQ cooler/buncher [10] of the ISOLTRAP Penning trap for precise mass measurements [11] at ISOLDE, CERN. Its aim is to decelerate, cool and bunch the continuous ISOLDE beam (60 keV energy,  $35\pi$  mm·mrad emittance) in order to deliver it with high efficiency to the first Penning trap for purification. This device is already working and has been used for mass measurements.
- The RFQ cooler [12] of the MISTRAL project [13] at ISOLDE, CERN, developed by CSNSM, Orsay. Its aim is to decelerate and cool the ISOLDE beam with the aim to improve the sensitivity of the MISTRAL mass spectrometer. The design and simulations of this system are completed and a prototype test version is being built at CSNSM.
- The RFQ cooler/buncher system for the CPT Penning trap mass spectrometer at Argonne [14]. The goal here is to stop the beam of recoiling nuclei coming out from a gas-filled recoil mass spectrometer and then to cool, bunch and eject them for precise nuclear mass measurements. The cooler/buncher system has been built. It was tested and proven to be fully operational [15].
- The RFQ cooler/buncher coupled to the IGISOL set-up at the Jyväskylä University. The goal here is to cool and bunch the radioactive ion beam coming out of the IGISOL set-up (energy spread about 100 eV, emittance about  $5\pi$  mm·mrad) to deliver it first to the purification Penning trap to reject the isobaric contaminant, and then to perform thereafter nuclear spectroscopy experiments. Collinear laser spectroscopy is also planned using the beam delivered by the cooler. Successful tests of the cooler have already been carried out and a transmission greater than 60% has been achieved [16].
- The SPIG (SextuPole Ion Guide) cooler has the same operating principle as the RFQ cooler except that a sextupole oscillating field is used to contain the ions instead of the

quadrupole one. Such devices are being used in combination with gas filled chambers, where reaction products are stopped in order to extract the ions of interest [17,18]. The quadrupole cooler has an advantage over the sextupole one since it is less complicated and delivers a narrower potential well in the transverse plane allowing a larger beam squeezing.

## **2.2 Buffer gas cooling with a Penning trap**

As mentioned above, there is another device that may be used for the cooling and bunching of a radioactive beam applying the buffer gas cooling technique: the Penning trap. The method has an additional great advantage: the cooling process may be done in a mass-selective way [8], reaching a mass resolving power of  $10^5$  [19], which allows to obtain an isobarically pure beam. A cooler/purifier Penning trap is working since long ago as a component of the ISOLTRAP set-up [19]. Another device of this type will start operating soon: the REX-trap Penning trap of the REX-ISOLDE radioactive beam project at CERN [20]. However, if there is no need to remove the isobaric contaminants from the beam, the RFQ cooler/buncher has advantages over the Penning trap: it is simpler and cheaper, it has shorter cooling times, it can accept higher beam intensities and it is easier to assure a higher transmission.

## **3. Description of the RFQ cooler/buncher**

### **3.1 Components of the set-up**

A schematic diagram of the main components of a beam handling system for an experiment using a Paul trap is shown in Fig. 1. The section with the RFQ cooler/buncher system is shown in Fig. 2. The set-up consists of three main parts: the deceleration section, the RFQ cooler/buncher itself and the extraction section. The three sections operate under different pressure conditions, what requires an efficient differential pumping.

### *The deceleration section*

Its aim is to decelerate the beam electrostatically to an energy of the order of 100 eV, which is relevant for injecting the ions into the RFQ ion guide. As mentioned above, this requires the positioning of part of the set-up on a high voltage platform that is at the same potential than the ion source, denoted as HV. In front of the ion guide, two electrodes should be placed. A first deceleration electrode of elliptical shape assures proper focusing conditions. The potential of this electrode should be about 1-3 kV below HV. A second focusing electrode, in the form of a thin disc, is maintained at some hundreds of volts below HV. This electrode serves also for the differential pumping. Both electrodes should focus the beam at the entrance of the RFQ cooler. In order to avoid voltage breakdowns the vacuum in this section should be better than  $10^{-2}$  Pa.

### *The RFQ cooler/buncher section*

The cooler may have one of the two configurations: open or closed. In the first case, the four rods are simply immersed in the buffer gas, which is contained in the chamber. The closed form requires sealing the spaces along the cooler axis between the neighboring rods and injecting the gas directly inside the structure. The latter solution is more complicated mechanically but is more beneficial from the differential pumping point of view. In order to achieve the axial guiding of ions towards the cooler exit, the rods should be divided, along the cooler axis, into segments, of about 1 to 5 cm length, separated by insulators. Appropriate DC voltages should be supplied to each segment, forming an electric field gradient which pushes the ions towards the exit. The segmentation can also be used to form the bunching section at the end of the cooler. To achieve this, the voltage supplied to a few segments of the exit end should form a potential well which confines the ions inside due to buffer gas collisions. After a certain time, the collected ions may be ejected out from the cooler in the form of a short bunch, by suddenly changing the potentials on the cooler rods. This procedure is necessary to inject the ions into the Paul trap with a high efficiency.

### *The extraction section*

The last section of the RFQ cooler/buncher is at the same time the injection section for the Paul trap. In order to be efficiently captured inside the Paul trap, the incoming ions should

have low energy, of typically few eV, allowing to stop them in the Paul trap center using a pulsed DC potential of moderate amplitude. A possible solution would be to put the Paul trap also on the HV platform but this makes the handling of experiments complicated. An alternative solution consists of:

- installing the Paul trap outside the HV platform, on the ground potential,
- placing between the HV platform and the Paul trap a cylindrical electrode, having initially the potential close to that of the HV platform, which may be pulsed down to zero,
- ejecting the ions from the RFQ cooler/buncher with low energy and adjusting this energy to the ground level by pulsing down the potential on the pulse-down electrode while the ions are in the center of this electrode.

The extraction section contains the following set of electrodes:

*a)* the extraction electrode, with the form of a thin disc. The potential of this electrode should be a few hundreds of volts below HV, which means that the electrode must be part of the HV platform. This electrode serves also as an aperture for the differential pumping in analogy to the focusing electrode.

*b)* the pulse-down electrode, described above, fixed at ground potential.

*c)* the transfer section, also at ground potential, which should contain a proper set of acceleration/deceleration/focusing electrodes, like Einzel lenses, delivering the ion bunch into the Paul trap.

A common requirement for the experiments is a high vacuum, in the range of  $10^{-7}$  Pa, to be present in the Paul trap region. This imposes the vacuum in the extraction section to be probably better than  $10^{-4}$  Pa, a strong requirement for the differential pumping.

### **3.2 Requirements for the buffer gas**

The cooling process can be made most effective and the effect of so called “RF-heating” which blows up the size of the ion cloud can be minimized if the buffer gas has a mass lighter, and preferably much lighter, than the ion mass [6]. This effect, which is inherent to the RF trap functioning, shows then up only in the presence of the buffer gas. The RF heating due to ion-ion collisions is usually negligible. The RF-heating mechanism is as follows: the ions, accelerated by the RF field, collide with the buffer gas molecules. After a collision there is a possibility that the ion ends up on a trajectory which is more distant from the RFQ cooler axis.



The probability depends on the energy, the velocity direction of the ion and the RF phase during which the collision occurs, and the new trajectory will correspond to a higher mean energy of the ion movement than the initial trajectory. In the worst case, the ion may be lost at the electrodes. To minimize the RF-heating effect, and to maximize the cooling effect, the ion momentum change has to be small at each collision. This happens when the ratio of the ion mass to the gas atom mass is large. If this ratio is close or less than 1 the cooling is no longer possible.

The buffer gas should have a low probability of charge exchange with the ion beam, and in particular an ionization potential higher than the atoms of interest, in order to minimize the losses of ions due to neutralization with the buffer gas. It should also be as pure as possible in order to avoid losses of ions due to neutralization with gas impurities. Usually the commercially available high purity gas should be sufficient. Finally, the gas should have a pressure sufficiently large in order to stop and cool the ions, but low enough to allow for the gas removal, by differential pumping.

There is no gas having higher ionization potential than helium ( $^4\text{He}$ ). At the same time, for many applications this gas fulfils the requirement for the mass relation. Therefore helium is generally used as buffer gas. However, such solution might not work efficiently for light mass beams and in particular for other He isotopes. For example,  $^6\text{He}^+$  in  $^4\text{He}$  will undergo a resonant charge exchange, which decreases the number of ions, and furthermore due to the small mass difference the RF-heating process may be significant.

## **4. Determination of the main RFQ cooler/buncher parameters**

### **4.1 Simulation methods**

The calculation of the main parameters of the system, like mechanical dimensions, voltages and pressures, may be done by means of computer simulations. There are several types of simulations treating differently the main interaction mechanisms between the ions and buffer gas atoms. These mechanisms are elastic collisions, inelastic collisions, and (resonant) charge exchange. In the energy regime of interest here, the inelastic collisions are

much less probable than the elastic ones and may therefore be neglected. Two main approaches exist, the so called *macroscopic* and the *microscopic*.

In the macroscopic approach the stopping and cooling of ions in the gas are treated on the average with the aid of the ion mobility concept [21]. Here, the drift velocity of an ion in the gas is proportional to the electric field acting on the ion:

$$v_d = \mu \cdot E,$$

where  $v_d$  is the ion drift velocity,  $\mu$  is the ion mobility and  $E$  the electric field. The effect of the average velocity dependent stopping force (viscous friction) can be described as the result of many elastic collisions with the gas atoms. That concept is relatively simple to implement in the ion trajectory calculations. In the absence of the electric field, the ion velocity is damped exponentially with time:

$$F_{vf} = (e/\mu) \cdot v_d, \quad \text{with} \quad v_d = v_0 \cdot \exp\{-te/(\mu m)\}$$

where  $t$  is the time parameter,  $m$  is the ion mass,  $e$  is the magnitude of the electron charge and  $F_{vf}$  is the viscous friction force. The value of  $e/(\mu m)$  is usually in a range of  $10^4 \text{ s}^{-1}$ .

This approach does not include the RF-heating phenomenon and should therefore be considered as a first approximation. Two computational methods exist. The fastest one relies on the numerical solution of the ion's equations of motion (Mathieu equations) assuming an ideal quadrupole potential. The other, which is much more memory and time consuming, simulates the ion motion in a realistic geometry, using the SIMION ion optics program.

If the cross section of the charge-exchange process is known, the process may also be accounted for in the macroscopic approach, by calculating the mean probability of ion neutralization in the gas at a given pressure.

In the microscopic approach the calculations treat each collision of the ion with the buffer gas atom separately, using a realistic potential for the ion-atom interaction of the so called (n,6,4) type [21,22]:

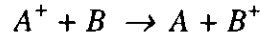


$$V(r) = \frac{B}{r^n} - \frac{C_6}{r^6} - \frac{C_4}{r^4}$$

where  $n = 8-16$ ;  $B$ ,  $C_4$  and  $C_6$  are constants, usually determined from experiment.

This approach inherently includes the RF-heating, and may also incorporate other processes like the charge-exchange reaction. Such calculations can be done by the Monte Carlo method and constitute a necessary second step of the full RFQ cooler simulations.

In the charge-exchange process:



a singly charged ion  $A^+$  may exchange an electron during a collision with a buffer gas atom or molecule  $B$  and get neutralized. A crucial point in the calculations is the knowledge of the charge-exchange cross section  $\sigma_{\text{chex}}$ . If the cross section is not known experimentally, one is forced to use a theoretical value. In the present study the dependence of the cross section on the ion kinetic energy is approximated by a constant above a given energy threshold  $E_{\text{thr}}$ . The value of the threshold is related to the first ionization potential of the projectile and buffer gas atoms (Fig. 3). To have a realistic estimate for  $\sigma_{\text{chex}}$  the calculations were done within a quantum-mechanical (QM) formalism [23]. The total Hamiltonian of the molecular ion, representing a full ion-atom system, can be expressed as:

$$H = H_e + T_N$$

where  $H_e$  stands for the electronic Hamiltonian in diabatic representation and  $T_N$  is the nuclear kinetic energy. A simplified reaction scheme with only one exit channel was adopted. This formalism was checked to give a reasonable agreement with selected experimental data for energies above 1 keV. Due to the simplicity of the interaction potentials used in these calculations, the results for the energy region below 1 keV should be interpreted rather in a qualitative manner. Nevertheless, the formalism may be used to predict reasonable limits for  $\sigma_{\text{chex}}$ .

## 4.2 Calculations

The estimate of the main parameters of the system has required several simulations of the deceleration and RFQ cooler sections which were performed with the two macroscopic ion mobility methods and with the microscopic approach. Such simulations are relatively complex and are done in an iterative way, where the output from an actual iteration serves as an input to the next one. Basically, the main aim is to find the best conditions for the beam cooling performing the optimization in the multidimensional space of parameters between which often some correlation exists. In the following, a procedure of finding the initial values for the most important parameters is outlined.

A closed RFQ cooler form was assumed to facilitate the differential pumping. The inputs of the simulations are: the value of the pressure inside the RFQ cooler,  $p_1$ , the pressure at the differential pumping orifices (inside the focusing electrode at the deceleration section and inside the extraction electrode at the extraction section),  $p_2$ , the cooler length  $L$  and inner radius  $r_0$ .

To avoid sparking at the deceleration region, the pressure  $p_2$  at both focusing and extraction electrodes was taken to be  $5 \cdot 10^{-3}$  Pa. The pressure  $p_1$  inside the RFQ cooler depends on both the inner diameters of the two orifices and the pumping speed.

The cooler length,  $L$ , should be on one hand as large as possible, to allow the stopping of ions of a given energy at the lowest possible pressure, thus permitting the lowest pumping speed. On the other hand, for practical reasons the length should not exceed 1 m, and so a cooler length of 70 cm (bunching section included) was assumed. With this length and with orifices diameters of 14 mm and two turbomolecular pumps with pumping speed of 1000 l/s each one obtains a pressure inside the cooler of  $p_1 = 0.1$  Pa.

The radius  $r_0 = 25$  mm was derived from the requirement that a beam with the  $80\pi$  mm-mrad emittance should be contained within the RFQ ion guide with no buffer gas inside.

The kinetic energy of the ions at the cooler entrance, of the order of 100 eV, can be adjusted to the energy at which the ions are stopped inside the cooler by selecting the proper potentials of the deceleration electrodes and the cooler rod segments.

The calculations are done in two steps. In the first step, the main cooler parameters are estimated within the macroscopic approach. These parameters serve as a starting point for the next phase: the microscopic calculations, with the aim to determine the cooling performances more precisely. The second step includes the charge exchange process. A constant charge-exchange cross section is assumed. Its value is chosen in such a way that the corresponding charge-exchange probability constitutes an upper limit. Due to this, the resulting transmission through the cooler represents a pessimistic, lower limit of the expected transmission. Whenever possible, the cross sections are taken from experiment, otherwise they are calculated theoretically within the quantum-mechanical formalism.

## 5. Results of the simulations

### 5.1 Macroscopic approach

The main result of these calculations was to prove that it is possible to decelerate a beam of 34 keV down to an energy of about 100 eV and inject it, with relatively high efficiency, inside the RFQ cooler. It is known that this approach is inaccurate for calculations of the cooling process inside the RFQ device, especially in the case when the ion mass is close to the buffer gas mass, because of the RF-heating phenomenon.

The reduction of the RF-heating effect is in principle possible by using a buffer gas other than helium. The only lighter gas is hydrogen, having the molecular mass  $A = 1$  ( $H_1$ ) or  $2$  ( $H_2$ ). However, due to the lower ionization potential of hydrogen, one may encounter also here some losses of  ${}^6\text{He}^+$  ions due to their neutralization, which will depend on the hydrogen pressure.

To summarize, the initial assumptions for the cooler simulations in the microscopic approach are the following (some of them result from the macroscopic calculations):

- ${}^6\text{He}^+$  beam energy (sharp):  $E_1 = 34$  keV,
- Beam emittance:  $\xi = 80 \pi$  mm·mrad,
- Beam entrance envelope as a plain ellipse (undistorted),
- RF voltage amplitude:  $V_{\text{RF}} = 250$  V (safe value in order to avoid breakdown),

- The Mathieu parameter  $q = 0.4$  (recommended value in order not to allow for the excessive RF distortion of the beam ellipse),
- RFQ cooler inner radius:  $r_0 = 25$  mm,
- RF voltage frequency:  $f = 900$  kHz (results from the adopted  $q$ ,  $r_0$  and  $V_{RF}$  values),
- RFQ cooler length:  $L = 70$  cm,
- Constant pressure  $p_1$  inside the cooler.

A schematic drawing of the set-up indicating the main parameters is shown in Fig. 4.

## 5.2 Microscopic approach

The simulations were performed using the Monte Carlo code developed at IKS Leuven [24], which allows to calculate the cooling of ions that undergo elastic collisions in the buffer gas. This code was extended in the present study to incorporate the charge-exchange process. The calculations use a realistic ion-atom interaction potential deduced from ion mobility data. In the frame of this approach, four different combinations have been investigated. The results are summarized in Table 1 and briefly discussed below:

- 1)  **${}^6\text{He}^+$  ions in  ${}^4\text{He}$  gas:**  $E_{\text{thr}} = 0$  eV,  $p_{\text{gas}} = 2$  Pa. The experimental value of  $\sigma_{\text{chex}} = 25 \cdot 10^{-20}$  m<sup>2</sup> [25] was used. The shape of the emittance at the cooler entrance was assumed as a plain ellipse (Fig. 5). The interaction potential was taken from the literature [26]. For a kinetic ion energy,  $E_{\text{ion}} = 20$  eV, at the cooler entrance the total transmission through the cooler *without charge exchange* amounts to  $\text{tr}(\text{tot}) = 67\%$  (Fig. 6) while a fraction of 33%, denoted as  $R_{\text{heat}}$ , is lost due to RF-heating. The transmission  $\text{tr}(\text{ell})$  within an elliptic output area ( $S_{\text{out}}/S_{\text{in}} = 0.074$ ) containing the cooled beam phase space amounts to 35%. The inclusion of the charge exchange process (resonant in this case), with a probability denoted as  $\text{chex}$ , decreases the transmission to  $10^{-38}$ . This means that, in practice, the cooling of  ${}^6\text{He}^+$  by  ${}^4\text{He}$  is not possible. The only way to decrease the charge-exchange probability is to decrease the gas pressure but then the cooling effect vanishes.

- 2)  **${}^6\text{He}^+$  ions in  $\text{H}_2$  gas:**  $E_{\text{thr}} = 0$  eV,  $p_{\text{gas}} = 3.3$  Pa. As an estimate of  $\sigma_{\text{chex}}$  a value of  $1 \cdot 10^{21}$   $\text{m}^2$  was assumed, which is an experimental cross section for  ${}^4\text{He}^+$  in  $\text{H}_1$  at 1 keV [27]. This assumption arises from the QM treatment which predicts that the cross section for  $\text{H}_2$  as buffer gas should be of similar order of magnitude than for  $\text{H}_1$ , and that the cross section for  ${}^6\text{He}^+$  in a given gas is always lower, than for  ${}^4\text{He}^+$ . In addition, the QM code predicts that the charge-exchange cross section should decrease with decreasing energy. The experimental data for  ${}^4\text{He}^+$  in  $\text{H}_2$  at the temperature of 500 K (0.043 eV) [28], yielding the charge-exchange cross section of about  $10^{-22}$   $\text{m}^2$ , are in agreement with our assumption. Due to the lack of ion mobility data for helium ions in hydrogen, the same interaction potential as for  $\text{Li}^+$  in  $\text{H}_2$  [29] was taken. This approximation should not be very far from reality since the collision integrals for different kinds of ions in  $\text{H}_2$  don't differ significantly. An example of an ion trajectory inside the cooler is shown in Fig. 7. For  $E_{\text{ion}} = 100$  eV, the total transmission through the cooler *without charge exchange* amounts to 62% (Fig. 8). The inclusion of (non-resonant) charge exchange, with the cross section indicated above, decreases this number to 21%. The transmission within the elliptic output area ( $S_{\text{out}}/S_{\text{in}} = 0.072$ ) amounts to 9%. It shows that in this case the cooling of a  ${}^6\text{He}^+$  beam seems to be feasible with a large transmission fraction.
- 3)  **${}^{40}\text{Ar}^+$  ions in  ${}^4\text{He}$  gas:**  $E_{\text{thr}} = 96.8$  eV,  $p_{\text{gas}} = 2$  Pa. Here, an upper limit of  $1 \cdot 10^{24}$   $\text{m}^2$  was taken for  $\sigma_{\text{chex}}$ , given by the QM treatment for a 10 keV energy. The code predicts the decrease of  $\sigma_{\text{chex}}$  with decreasing energy. The ion-atom interaction potential was derived from the ion mobility data [29]. For  $E_{\text{ion}} = 100$  eV, the total transmission through the cooler without charge-exchange effect amounts to 96% (Fig. 9). Including the charge exchange process causes an additional loss of ions at the level of  $10^{-4}$  of their original number, which shows that the charge exchange plays here virtually no role.
- 4)  **${}^{100}\text{Sn}^+$  ions in  ${}^{40}\text{Ar}$  gas:**  $E_{\text{thr}} = 29.5$  eV,  $p_{\text{gas}} = 0.4$  Pa. The QM theoretical cross section at 10 keV energy amounts to  $1 \cdot 10^{27}$   $\text{m}^2$  and was taken as an upper limit for  $\sigma_{\text{chex}}$ . Similarly, in the absence of ion mobility data for  $\text{Sn}^+$  in Ar, the mobility for  $\text{Cs}^+$  in Ar [30] was adopted for the determination of the interaction potential. For  $E_{\text{ion}} = 100$  eV,

the total transmission through the cooler without charge exchange amounts to 47% (Fig. 10). The inclusion of the charge exchange process has also no effect in this case.

Table 1

| ion                   | $E_{\text{ion}}$<br>[eV] | gas                | $p_{\text{gas}}$<br>[Pa] | $E_{\text{thr}}$<br>[eV] | $\sigma_{\text{chex}}$<br>[ $10^{-20}$<br>$\text{m}^2$ ] | RF-heat<br>[%] | chex<br>[%] | tr(ell)<br>[%] | tr(tot)<br>[%] |
|-----------------------|--------------------------|--------------------|--------------------------|--------------------------|--|----------------|-------------|----------------|----------------|
| ${}^6\text{He}^+$     | 20                       | ${}^4\text{He}$    | 2                        | $\infty$                 | 0  | 33             | 0           | 35             | 67             |
| ${}^6\text{He}^+$     | 20                       | ${}^4\text{He}$    | 2                        | 0                        | 25   | 0              | 100         | 0              | 0              |
| ${}^6\text{He}^+$     | 100                      | $\text{H}_2$       | 3.3                      | $\infty$                 | 0  | 38             | 0           | 27             | 62             |
| ${}^6\text{He}^+$     | 100                      | $\text{H}_2$       | 3.3                      | 0                        | 0.1  | 34             | 45          | 9              | 21             |
| ${}^{40}\text{Ar}^+$  | 100                      | ${}^4\text{He}$    | 2                        | $\infty$                 | 0  | 4              | 0           | 74             | 96             |
| ${}^{40}\text{Ar}^+$  | 100                      | ${}^4\text{He}$    | 2                        | 96.8                     | $10^{-4}$  | 4              | 0           | 74             | 96             |
| ${}^{100}\text{Sn}^+$ | 100                      | ${}^{40}\text{Ar}$ | 0.4                      | $\infty$                 | 0  | 53             | 0           | 25             | 47             |
| ${}^{100}\text{Sn}^+$ | 100                      | ${}^{40}\text{Ar}$ | 0.4                      | 29.5                     | $10^{-7}$  | 53             | 0           | 25             | 47             |

## 6. Optimization of the RFQ cooler dimensions

As shown in the previous section, it should be possible to cool a  ${}^6\text{He}^+$  beam in  $\text{H}_2$  buffer gas, in a cooler of inner radius  $r_0 = 25$  mm and length  $L = 70$  cm. However, these dimensions, and particularly the radius, are relatively large. This may cause problems for the efficient differential pumping and also for finding an RF amplifier having the required power. On the other hand, the emittance of the beam delivered by the ion source to be used for an actual experiment might be smaller than  $80\pi$  mm·mrad at 34 keV. Therefore, as a compromise between the cooler transmission and the limitation of technical problems, it was advised to decrease the cooler dimensions. In this aim, the calculations for  ${}^6\text{He}^+ + \text{H}_2$  case were done assuming a cooler of  $r_0 = 10$  mm radius and  $L = 50$  cm length. These calculations have shown that for the same entrance conditions as before, ( $E_{\text{thr}} = 0$  eV,  $p_{\text{gas}} = 2.5$  Pa,  $\sigma_{\text{chex}} = 1 \cdot 10^{-21}$  m<sup>2</sup>



and  $E_{ion} = 100$  eV), the transmissions through the elliptic cooled beam area amount to 13% and 8%, for initial beam emittances of  $32\pi$  and  $80\pi$  mm-mrad, respectively. The corresponding transmission figures in the absence of charge exchange, which provide an upper transmission limit, are 26% and 18%, respectively.

## 7. Discussion of the cooler parameters

The set of parameter presented in section (4.2) is of course not unique but provides a possible configuration. The parameters and the relations between them are briefly discussed below:

1. The inner cooler radius  $r_0$ , which is related to the rod radius  $r_{rod} = 1.148 \cdot r_0$  [31], is mainly determined by the beam emittance, both in value and shape. A larger emittance results in a larger radius.
2. The cooler length  $L$  increases with the ion kinetic energy  $E_1$  at the cooler entrance and decreases with the buffer gas pressure  $p_1$ . It is thus dependent on the pumping speed.
3. The buffer gas pressure inside the cooler,  $p_1$ , depends on the diameter of the differential pumping apertures diameter  $d_2$ , on the cooler radius  $r_0$ , on the length  $L$ , and on the pressure at the high vacuum side of the orifices  $p_2$ . Due to the upper limit of the pumping speed and of the pressure  $p_2$  (voltage breakdown), there is an upper limit for the achievable pressure  $p_1$ , with a given radius  $r_0$ . In general, this pressure should be maximized to obtain a faster cooling and to decrease the cooler length  $L$ , paying attention that, simultaneously, the ion propagation time through the cooler stays at an acceptable level.
4. The diameter of the aperture  $d_2$  for the differential pumping depends on the beam size at each end. For simplicity, the same diameter was assumed at both ends of the cooler. In the final set-up smaller diameter could be adopted at the extraction side, since the beam diameter should be there much smaller than at the injection side. In general, this diameter should be minimized to increase the efficiency of the differential pumping.
5. The initial energy of the beam,  $E_0 = 34$  keV, should be varied within the whole range of possible energies available at the ion source.

6. A beam emittance of  $\xi = 80\pi$  mm·mrad was assumed in the calculations but smaller values are expected for some ion sources.
7. The shape of the beam at the entrance, as an undistorted plain ellipse, should have to be changed.
8. The kinetic energy of the ions at the cooler entrance,  $E_1$ , may be varied within some hundreds of eV, but generally should be minimized in order to reduce the ion beam divergence, and possible losses, due to collisions with buffer gas at the cooler entrance.
9. The optimal of the RF voltage amplitude should be adjusted experimentally.
10. The optimal value of the Mathieu parameter  $q$  should also be adjusted experimentally.
11. The pressure at the focusing and extraction electrodes,  $p_2 = 5 \cdot 10^{-3}$  Pa, has to be verified experimentally. The possibility to work at a higher pressure, without sparking, should be considered.

## 8. Conclusion

This study has shown that the buffer gas cooling technique using an RFQ ion guide can be extended to the case of light ions. In particular, it was demonstrated that the cooling of a beam of  ${}^6\text{He}^+$  ions could be achieved, with a significant transmission, using  $\text{H}_2$  as buffer gas. For the first time the charge-exchange collisions have been incorporated in the simulations of the cooling process. The charge-exchange cross sections were either calculated within a quantum mechanical formalism or taken from experiment whenever available. A set of design parameters for an RFQ cooler and buncher system has been proposed and the relations between them have been discussed. The performance of the RFQ system has been calculated in different approaches for several combinations of beam ions/buffer gas atoms.

*This work has been performed in the framework and with the support of the EXOTRAPs RDT Network (contract ERBFMG CETY 980099) and in collaboration with IKS Leuven, CSNSM Orsay and ISOLDE CERN.*

## Figure captions

**Fig. 1:** Block diagram of a typical experiment.

**Fig. 2:** Block diagram of the RFQ cooler/buncher set-up.

**Fig. 3:** Model for the energy dependence of the charge-exchange cross section,  $\sigma_{\text{chex}}$ :  $E_{\text{ion}}$  is the ion kinetic energy,  $E_{\text{thr}}$  is the ion threshold energy,  $I_{\text{ion}}$  (resp.  $I_{\text{gas}}$ ) is the first ionization potential of the beam (resp. buffer gas) atoms,  $m_{\text{ion}}$  (resp.  $m_{\text{gas}}$ ) is the mass of the beam ion (resp. buffer gas atom).

**Fig. 4:** A schematic drawing of the RFQ cooler, indicating its main parameters. Inset: view of the transverse section of the cooler.

**Fig. 5:** Shape of the beam emittance at the entrance for  ${}^6\text{He}^+$  at  $E_{\text{ion}} = 20$  eV. The area corresponds to  $80\pi$  mm · mrad at 34 keV. The axes denote the spatial coordinate and velocity in the transverse plane.

**Fig. 6:** Shape of the beam emittance for  ${}^6\text{He}^+$  in  ${}^4\text{He}$  buffer gas,  $E_{\text{ion}} = 20$  eV, buffer gas pressure  $p = 2$  Pa (simulation for 5041 ions). The area circumscribed by the ellipse, indicating the reduction of the emittance, corresponds to 0.072 of the value of emittance at the entrance. The transmission within this area amounts to 35%. A fraction of 33% of ions is lost due to the RF-heating.

**Fig. 7:** Example of a trajectory of an ion (axial versus transverse coordinate) inside the RFQ cooler for the case of  ${}^6\text{He}^+$  ions in  $\text{H}_2$  gas, with  $E_{\text{ion}} = 100$  eV,  $p = 3.3$  Pa, and no charge exchange.

**Fig. 8:** Shape of the beam emittance at the RFQ exit (same conditions as Fig.7).

**Fig. 9:** Shape of the beam emittance at the RFQ exit for  ${}^{40}\text{Ar}^+$  ions in  ${}^4\text{He}$  gas, with  $E_{\text{ion}} = 100$  eV,  $p = 2$  Pa, and no charge exchange.

**Fig. 10:** Shape of the beam emittance at the exit for  ${}^{100}\text{Sn}^+$  ions in  ${}^{40}\text{Ar}$  gas, with  $E_{\text{ion}} = 100$  eV,  $p = 0.4$  Pa, and no charge exchange.

## References

- [1] G. Ban *et al.*, LPC internal report LPCC-99-16, unpublished
- [2] D. Möhl *et al.*, *Phys. Rep.* **58** (1980) 73
- [3] H. Poth, *Phys. Rep.* **196** (1990) 135
- [4] D. A. Church and H. G. Dehmelt, *J. Appl. Phys.* **40** (1969) 3421
- [5] F. Diedrich *et al.*, *Phys. Rev. Lett.* **59** (1987) 2931
- [6] F. G. Major and H. G. Dehmelt, *Phys. Rev.* **170** (1968) 91
- [7] M.D. Lunney, F. Buchinger and R.B. Moore, *J. Mod. Optics* **39** (1992) 349
- [8] M. König *et al.*, *Int. J. Mass Spectrom. Ion Proc.* **142** (1995) 95
- [9] D.J. Douglas and J.B. French, *J. Am. Soc. Mass Spectrom.* **3** (1992) 398
- [10] G. Bollen *et al.*, in Proc. of the 2<sup>nd</sup> Int. Conf. on Exotic Nuclei and Atomic Masses (ENAM98), Bellaire, USA, 1998.
- [11] G. Bollen *et al.*, *Nucl. Instr. Meth. in Nucl. Res.* **A368** (1996) 675
- [12] M.D. Lunney and R.B. Moore, *Int. J. Mass Spectrom.* **190/191** (1999) 153
- [13] Mass measurements at ISOLDE using a Transmission RADIO-frequency spectrometer on-Line (IS-346): see M.D. Lunney *et al.*, *Hyp. Int.* **99** (1996) 105 and M. de Saint Simon *et al.*, *Phys. Scripta* **T59** (1995) 406
- [14] G. Savard *et al.*, *Nucl. Phys.* **A626** (1997) 353c
- [15] G. Savard, private communication (1999)
- [16] J. Äystö, private communication (1999)
- [17] P. Van den Bergh *et al.*, *Nucl. Instr. Meth. in Nucl. Res.* **B126** (1996) 194
- [18] H.J. Xu *et al.*, *Nucl. Instr. Meth. in Nucl. Res.* **A333** (1993) 274
- [19] H. Raimbault-Hartmann *et al.*, *Nucl. Instr. Meth. in Nucl. Res.* **B126** (1997) 378
- [20] D. Habs *et al.*, *Nucl. Instr. Meth. in Nucl. Res.* **B126** (1997) 218
- [21] E. A. Mason and E. W. McDaniel, *Transport properties of ions in gases*, J. Wiley & Sons, New York, 1988
- [22] L. A. Viehland *et al.*, *At. Nucl. Data Tables* **16** (1975) 495
- [23] R. McCarroll and P. Valiron, *Astron. Astrophys.* **53** (1976) 83
- [24] B. Bruyneel, private communication (1999) and Rapport d'activité I.I.S.N. et U.C.L.-Louvain-la-Neuve, 1998, p.65
- [25] M. V. V. S. Rao *et al.*, *Phys. Rev.* **E54** (1996) 5641
- [26] A. S. Dickinson, *J. Phys.* **B1** (1968) 387
- [27] C. Harel and A. Salin, *J. Phys.* **B16** (1983) 55
- [28] M. Kimura and N. F. Lane, *Phys. Rev.* **A44** (1991) 259
- [29] H. W. Ellis *et al.*, *At. Nucl. Data Tables* **17** (1976) 177
- [30] H. W. Ellis *et al.*, *At. Nucl. Data Tables* **22** (1978) 179
- [31] P. H. Dawson, *Quadrupole mass spectrometry and its applications*, Elsevier Sci. Publishing Co., Amsterdam (1976)



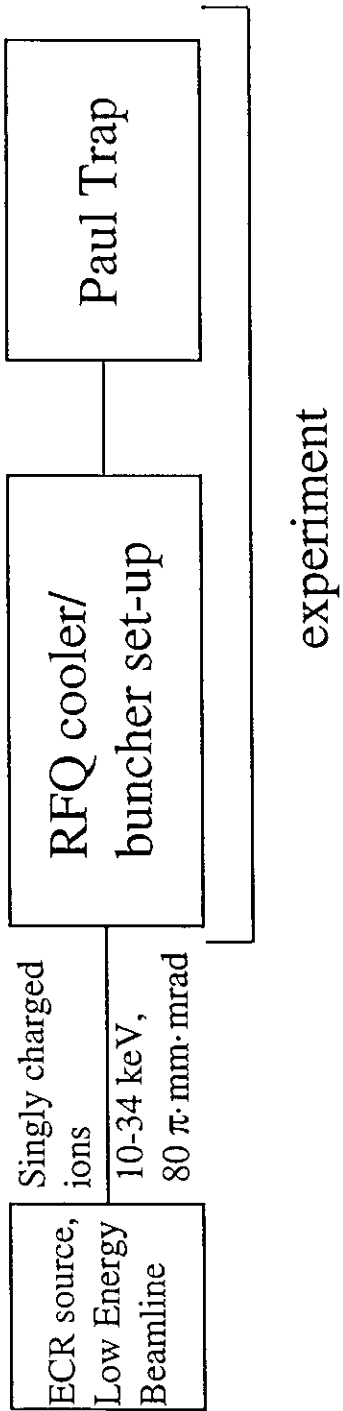


Fig. 1

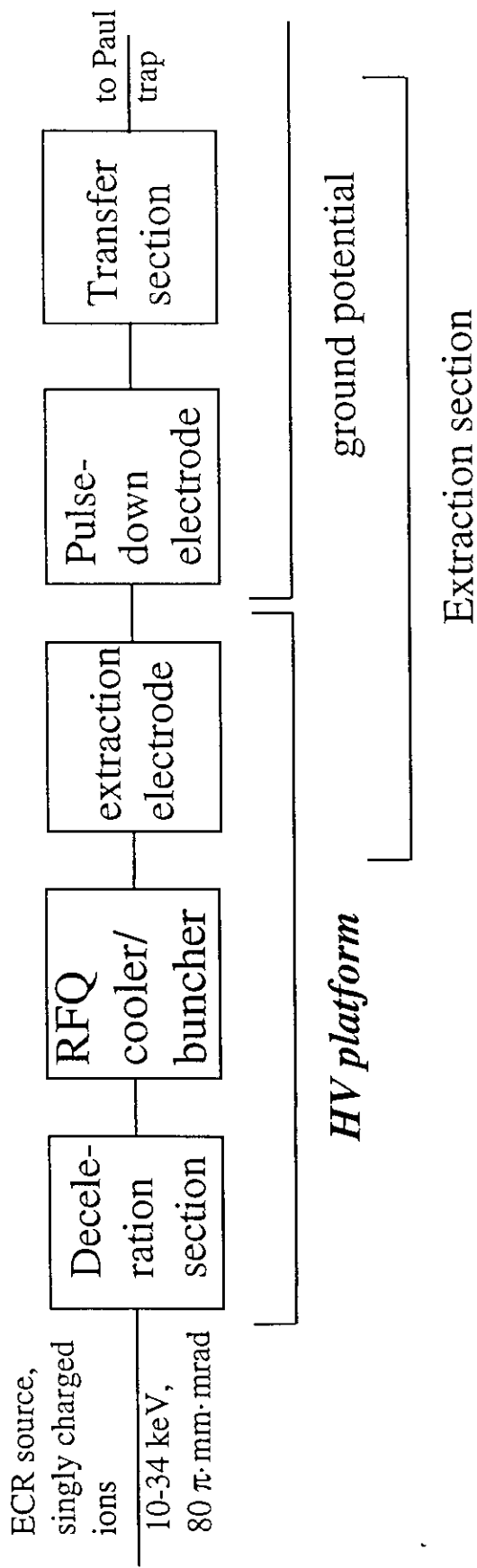
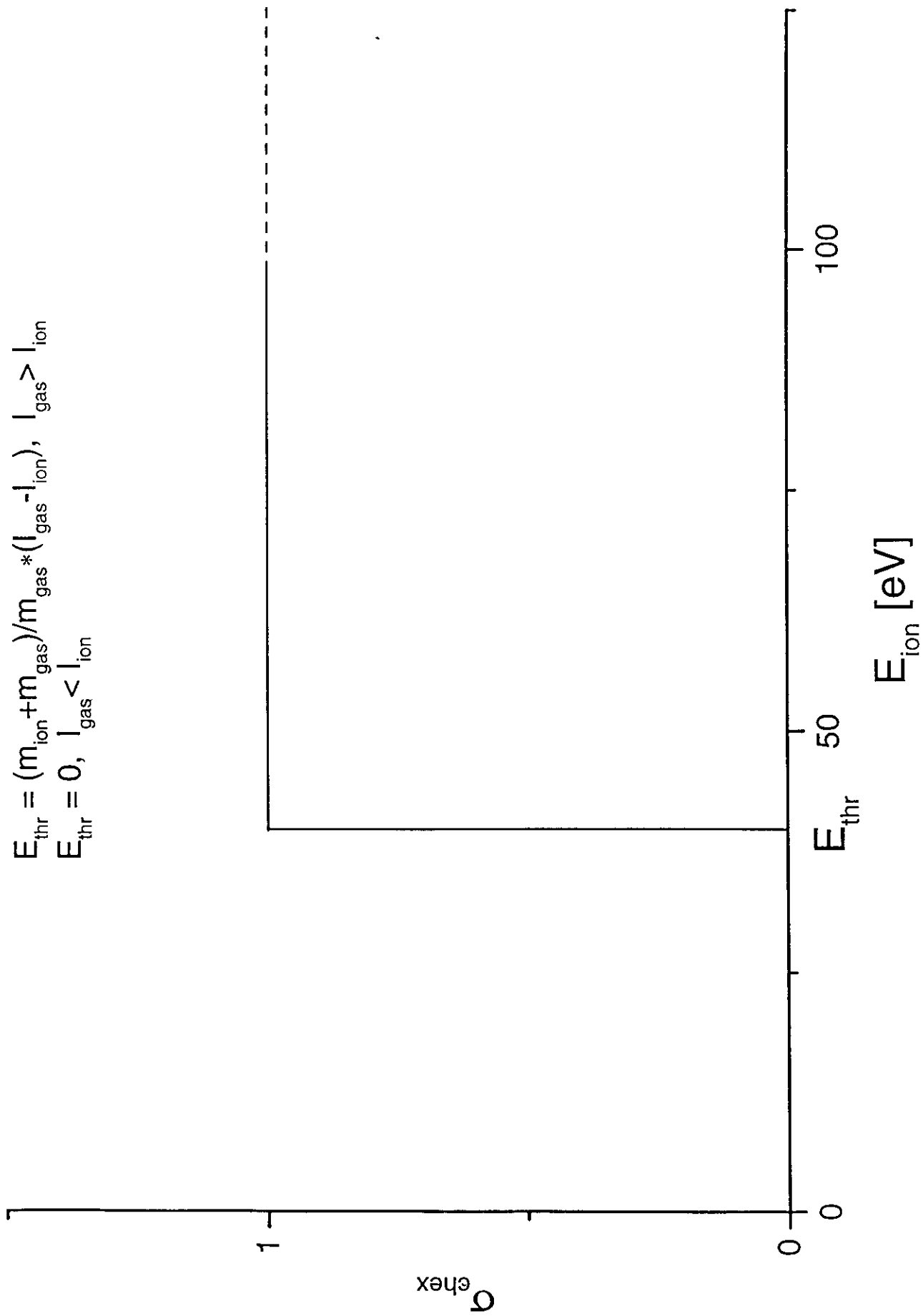


Fig. 2

$$E_{\text{thr}} = (m_{\text{ion}} + m_{\text{gas}}) / m_{\text{gas}} * (I_{\text{gas}} - I_{\text{ion}}), \quad I_{\text{gas}} > I_{\text{ion}}$$

$$E_{\text{thr}} = 0, \quad I_{\text{gas}} < I_{\text{ion}}$$



RFQ ion guide

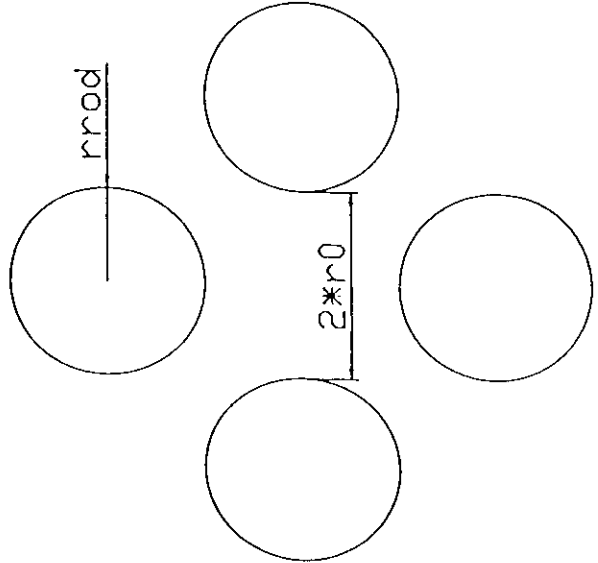
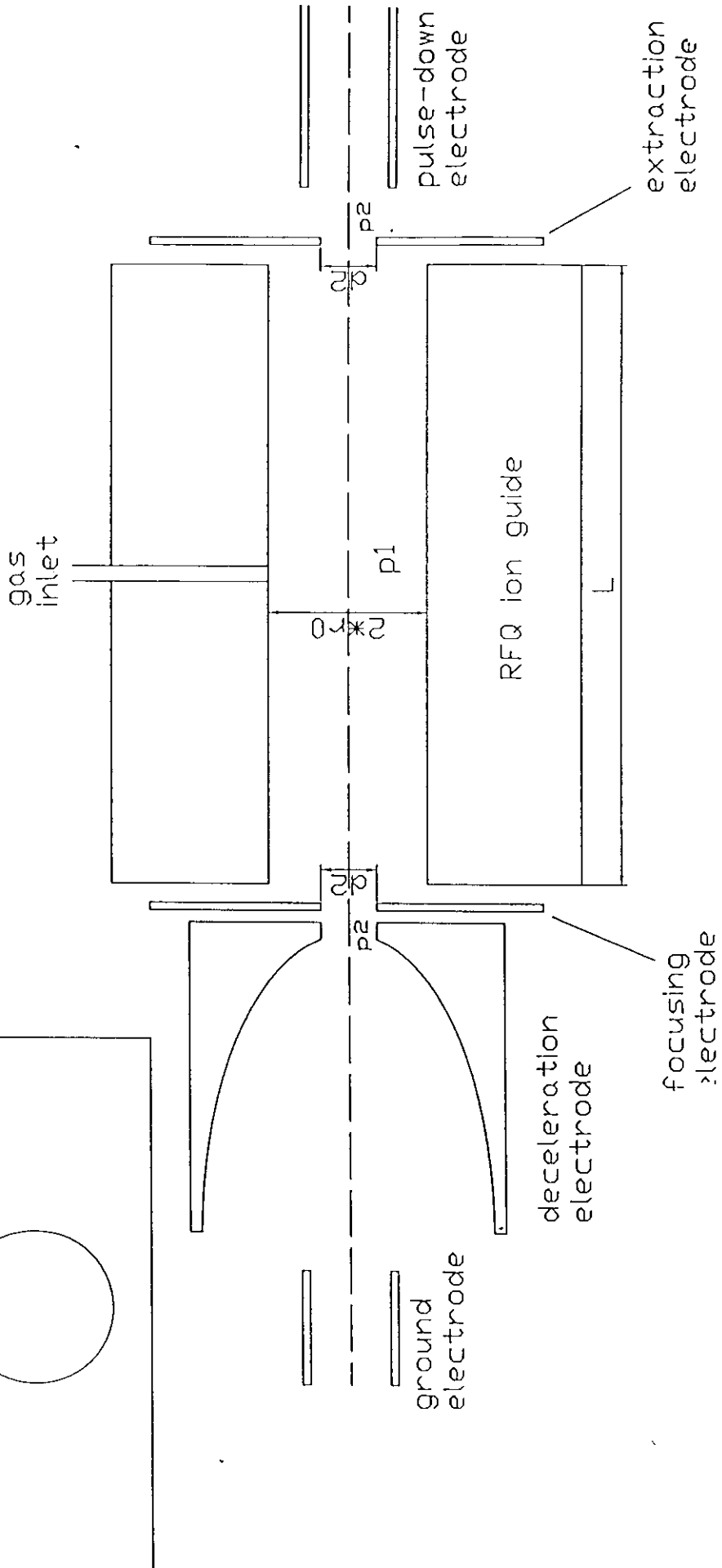


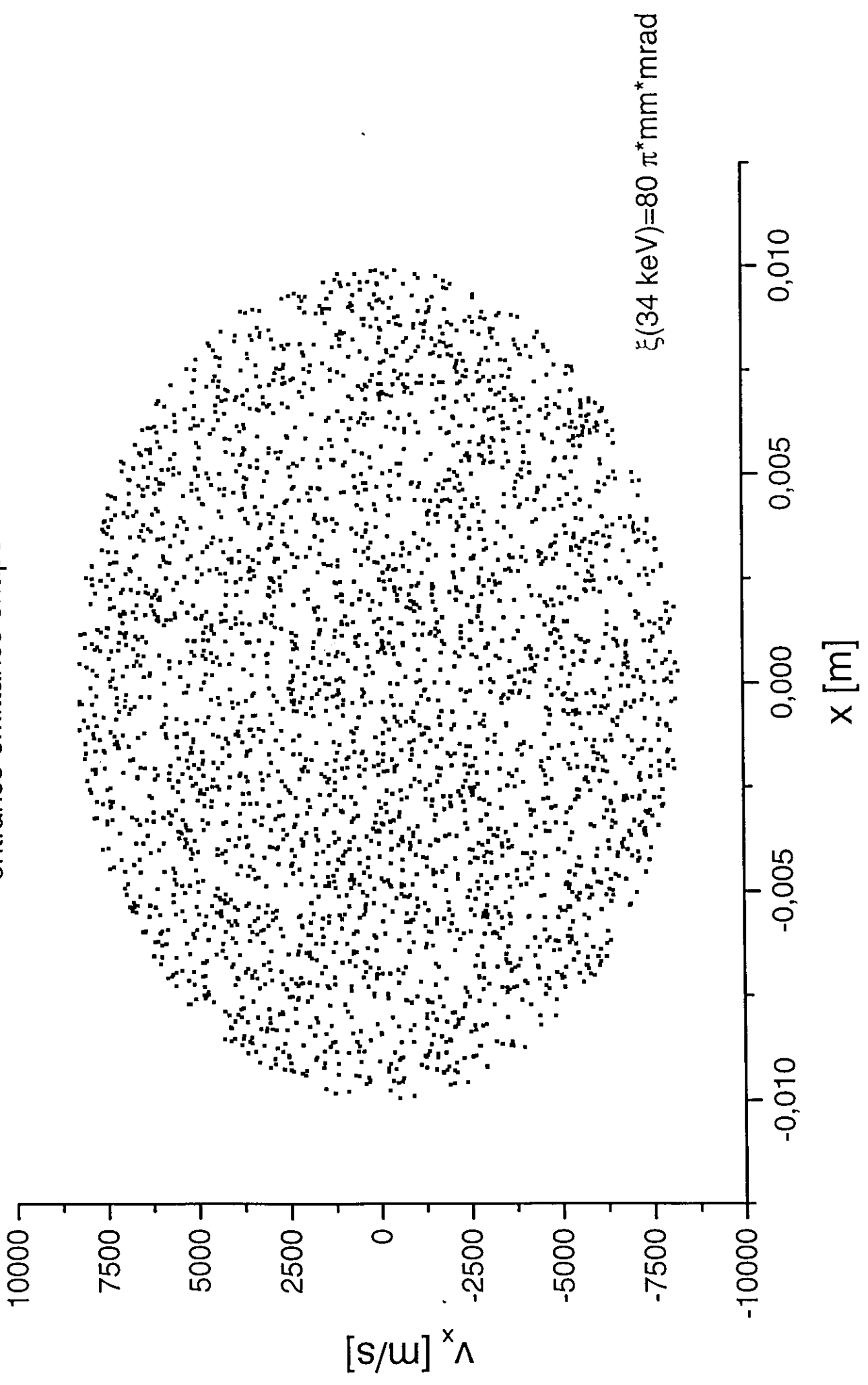
fig.4





${}^6\text{He}^+$  in  ${}^4\text{He}$ ,  $E_{\text{kin}}=20\text{ eV}$

entrance emittance shape



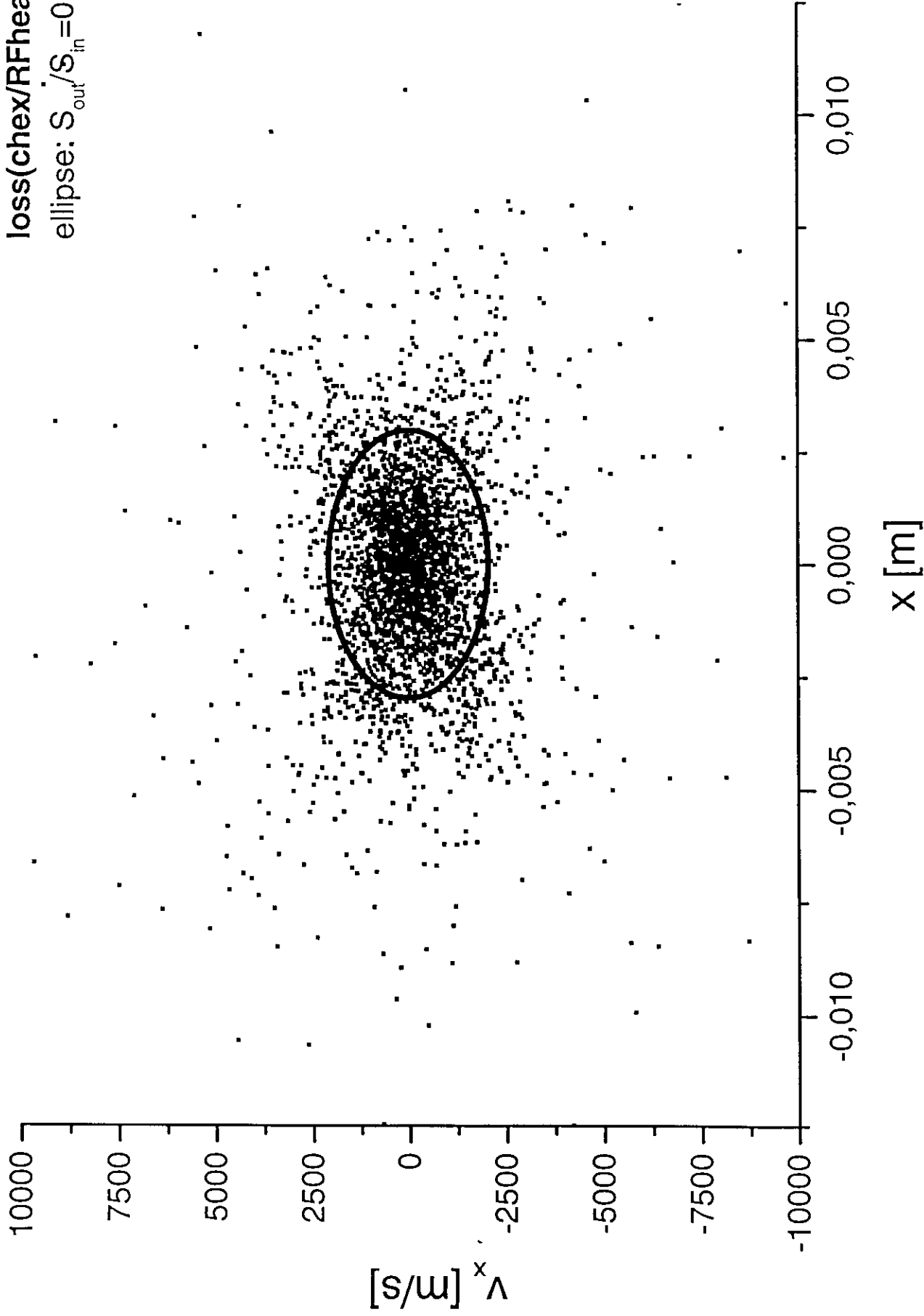
${}^6\text{He}^+$  in  ${}^4\text{He}$ ,  $p=2$  Pa  
 $E_{\text{kin}}=20$  eV,  $\sigma_{\text{chex}}=0$

ion=5041

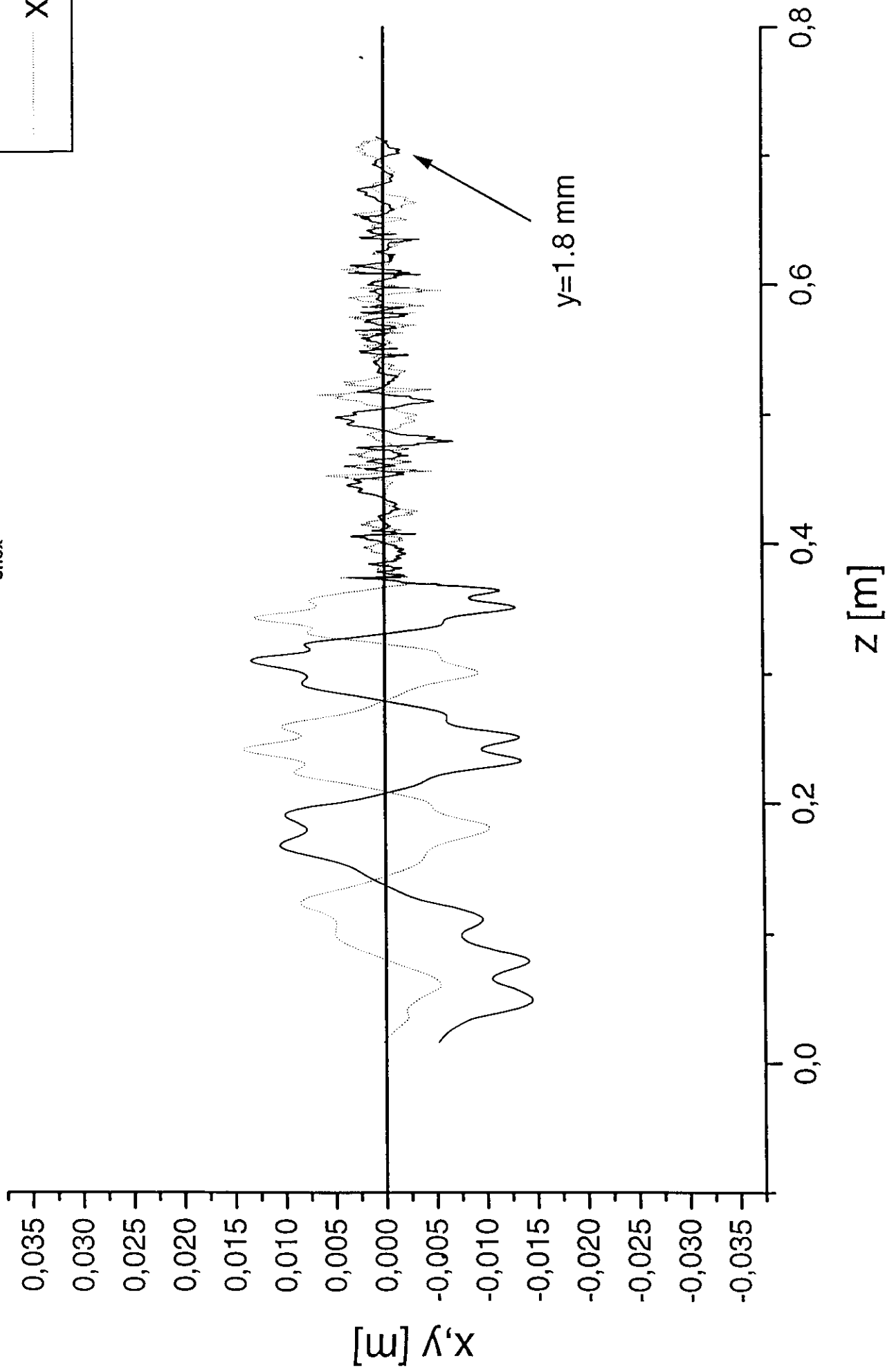
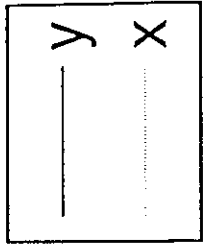
tr(tot/ell)=67/35%

loss(chex/RFheat)=0/33%

ellipse:  $S_{\text{out}}/S_{\text{in}}=0.072$



${}^6\text{He}^+$  in  $\text{H}_2$ ,  $p=3.3\text{ Pa}$   
 $E_{\text{kin}}=100\text{ eV}$ ,  $\sigma_{\text{chex}}=0$



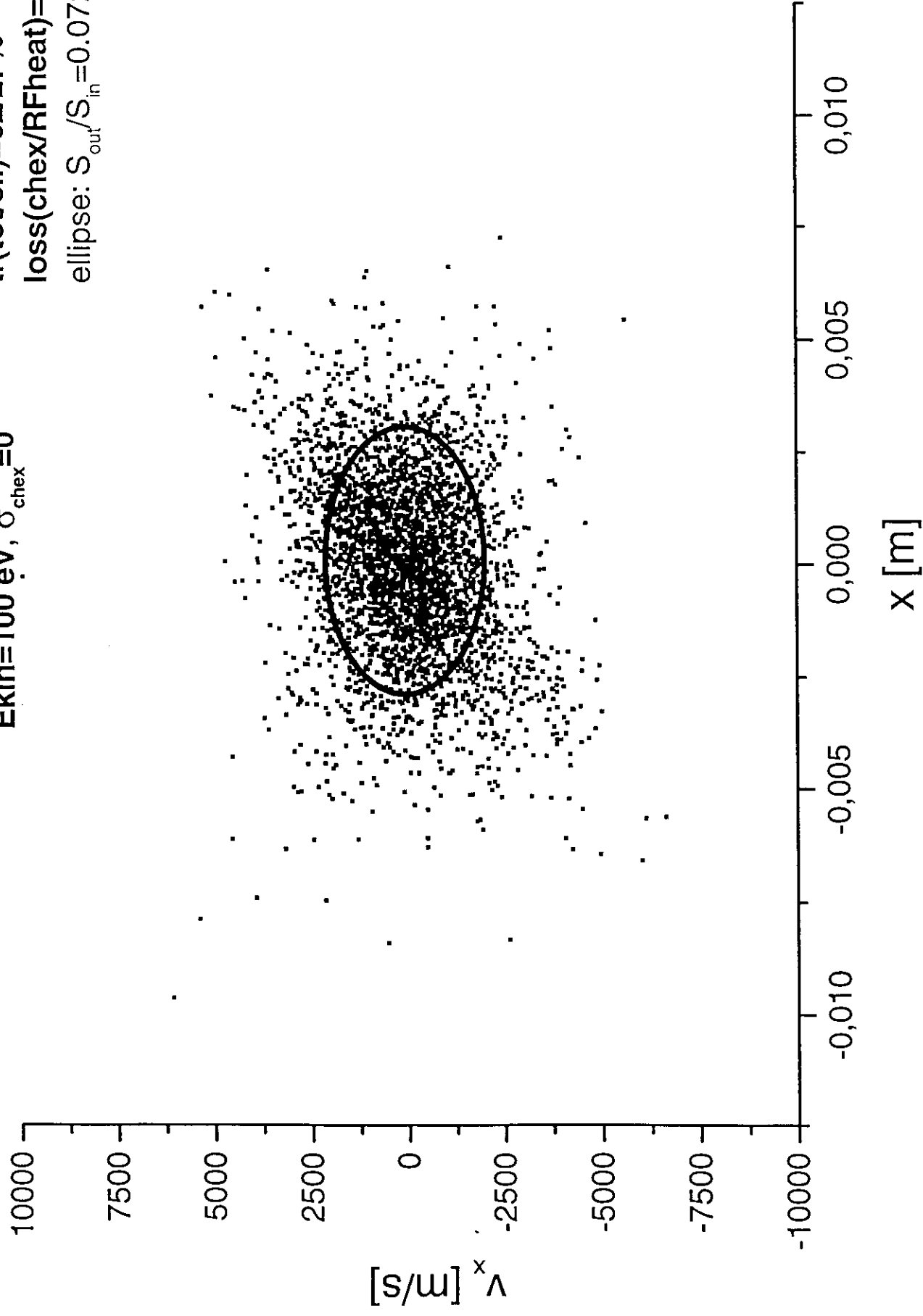
${}^6\text{He}^+$  in  $\text{H}_2$ ,  $p=3.3$  Pa  
 $E_{\text{kin}}=100$  eV,  $\sigma_{\text{chex}}=0$

ion=5772

tr(tot/ell)=62/27%

loss(chex/RFheat)=0/38%

ellipse:  $S_{\text{out}}/S_{\text{in}}=0.072$



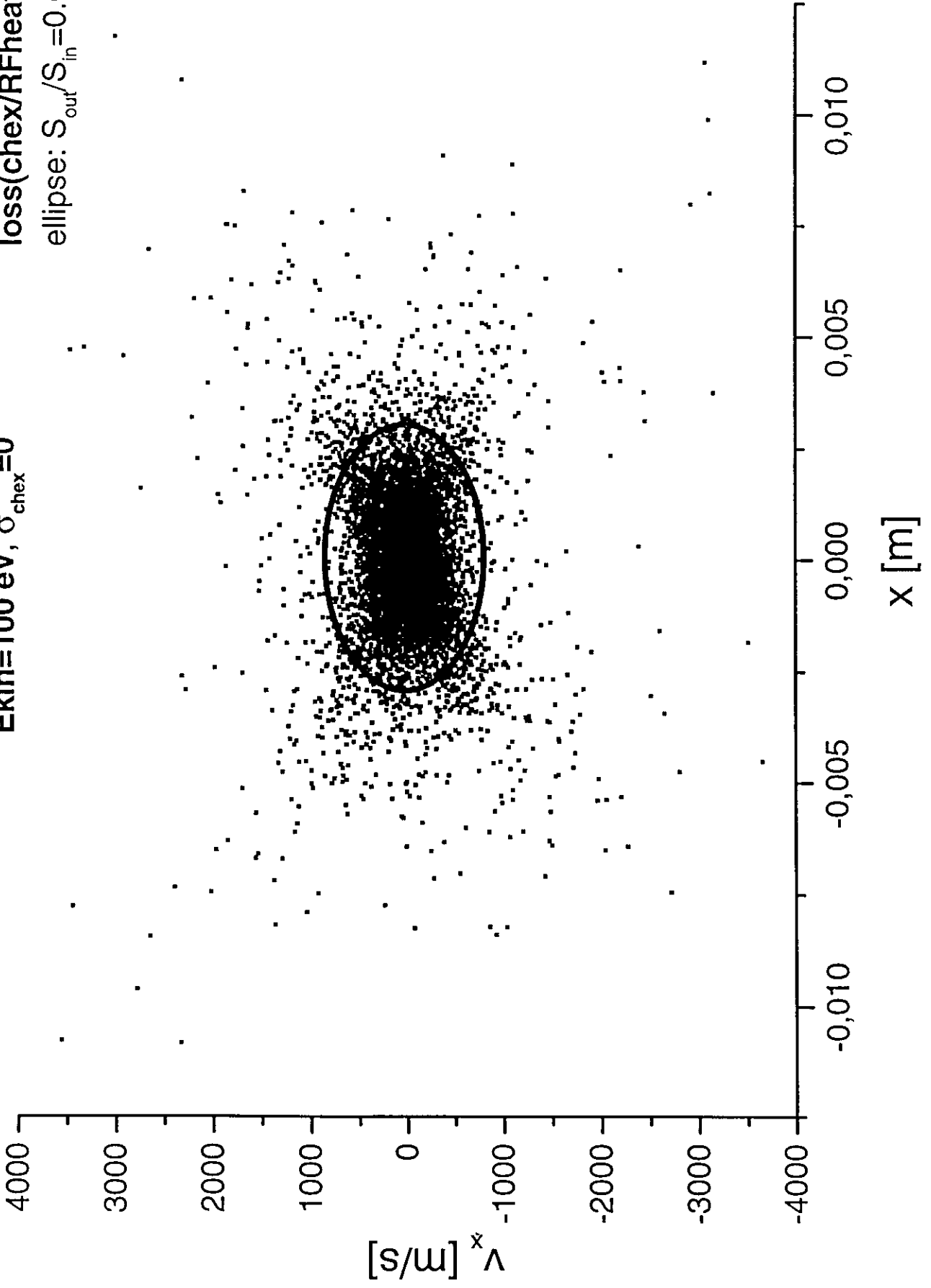
$^{40}\text{Ar}^+$  in  $^4\text{He}$ ,  $p=2$  Pa  
 $E_{\text{kin}}=100$  eV,  $\sigma_{\text{chex}}=0$

ion=7969

tr(tot/ell)=96/74%

loss(chex/RFheat)=0/4%

ellipse:  $S_{\text{out}}/S_{\text{in}}=0.074$



$^{100}\text{Sn}^+$  in  $^{40}\text{Ar}$ ,  $p=0.4\text{ Pa}$

$E_{\text{kin}}=100\text{ eV}$ ,  $\sigma_{\text{chex}}=0$

ion=10000

tr(tot/ell)=47/25%

loss(chex/RFheat)=0/53%

ellipse:  $S_{\text{out}}^*/S_{\text{in}}=0.074$

